engineering proceedings

MDPI

Proceeding Paper

Analysis of the Gabčíkovo Lock Outlet Channel Failure †

Miloš Zich [1,*], Michael Trnka [2], Ondřej Šimek [1] and Martin Lukšo [1]

[1] Faculty of Civil Engineering, Brno University of Technology, 602 00 Brno, Czech Republic; ondrej.simek2@vut.cz (O.Š.); martin.lukso@vut.cz (M.L.)
[2] Aquatis, a.s., 602 00 Brno, Czech Republic; michael.trnka@aquatis.cz
* Correspondence: milos.zich@vut.cz; Tel.: +420-5114-7860
† Presented at the 15th Central European Congress on Concrete Engineering (CCC2026), Vodice, Croatia, 5–7 October 2026.

Abstract

The paper presents the results of an analysis of the causes of failure of the concrete walls in the outflow channels of the Gabčíkovo lock chambers. The waterworks is located on the Danube River approximately 60 km southeast of Bratislava, the capital of Slovakia. It consists of two locks. The lock chambers are among the largest in the world. The usable length of one lock is 275 m, and its width is 34 m. Each lock is equipped with four outlet channels, each with a cross-section of 4 × 4 m. The channels consist of 2.0 m thick concrete walls and slabs. During operation, they are subjected to hydrostatic pressure corresponding to a water head of up to 30 m. During the reconstruction of the lock in 2019–2023, extensive damage was discovered in these walls at the wall-to-slab construction joints. The paper presents a detailed nonlinear analysis and a proposed strengthening solution.

Keywords: reinforced concrete; lock chamber; structural failure; nonlinear analysis

1. Introduction

This paper follows previous studies describing the complete reconstruction of the Gabčíkovo lock on the Danube River [1,2] and focuses on the analysis of the failure of the outflow channels.

The waterworks comprises two locks of identical dimensions. The usable length of one lock is 275 m, with a width of 34 m and wall height of 30 m (Figures 1 and 2). Depending on the water levels, the hydraulic head across the lock ranges from 12.7 m to 23.6 m. The lock consists of an upper block with a gate, six approximately 45 m long dilatation blocks forming the lock chamber, and a lower block with a gate. The chambers are connected to the inlet and outlet structures by a system of filling and emptying channels.

From a structural point of view, a typical section of the chamber forms a reinforced concrete half-frame. The upper block is a massive concrete structure, while the lower block is a frame with a transverse connection in the form of a reinforced concrete bridge between the walls. The concrete structures of the chamber were designed in 1985–1987 [3]. Concrete class 250 (equivalent to the current strength class C16/20 [4]) and reinforcing steel with f_{yk} = 425 MPa were used. Large-diameter reinforcing bars of 40 and 50 mm were frequently used, with concrete cover reaching up to 150 mm.

The upper and lower blocks of the chamber are fitted with movable gates. The lower gate is a steel plate-type gate consisting of two halves, each measuring 19.6 × 22 m and weighing approximately 460 t. The total weight of the lower gate is therefore 920 t, with an additional 160 t of associated steel structures, including components embedded in the

Check for updates

Academic Editors: Josip Galić, Jelena Bleiziffer, Davor Andrić and Vita Varezić

Published: 27 October 2026

Copyright: © 2026 by the authors. Licensee MDPI, Basel, Switzerland. This article is an open access article distributed under the terms and conditions of the Creative Commons Attribution (CC BY) license.

bearing blocks and sealing elements. The upper block is fitted with a segmental steel gate measuring approximately 11 × 34 m and weighing approximately 310 t. In addition, a steel back-up safety flap gate measuring 8.9 × 34 m and weighing 170 t is installed in the upper block. The original flap consisted of two separate parts.



Figure 1. Aerial view of the lock chambers and the dam of the artificial canal.

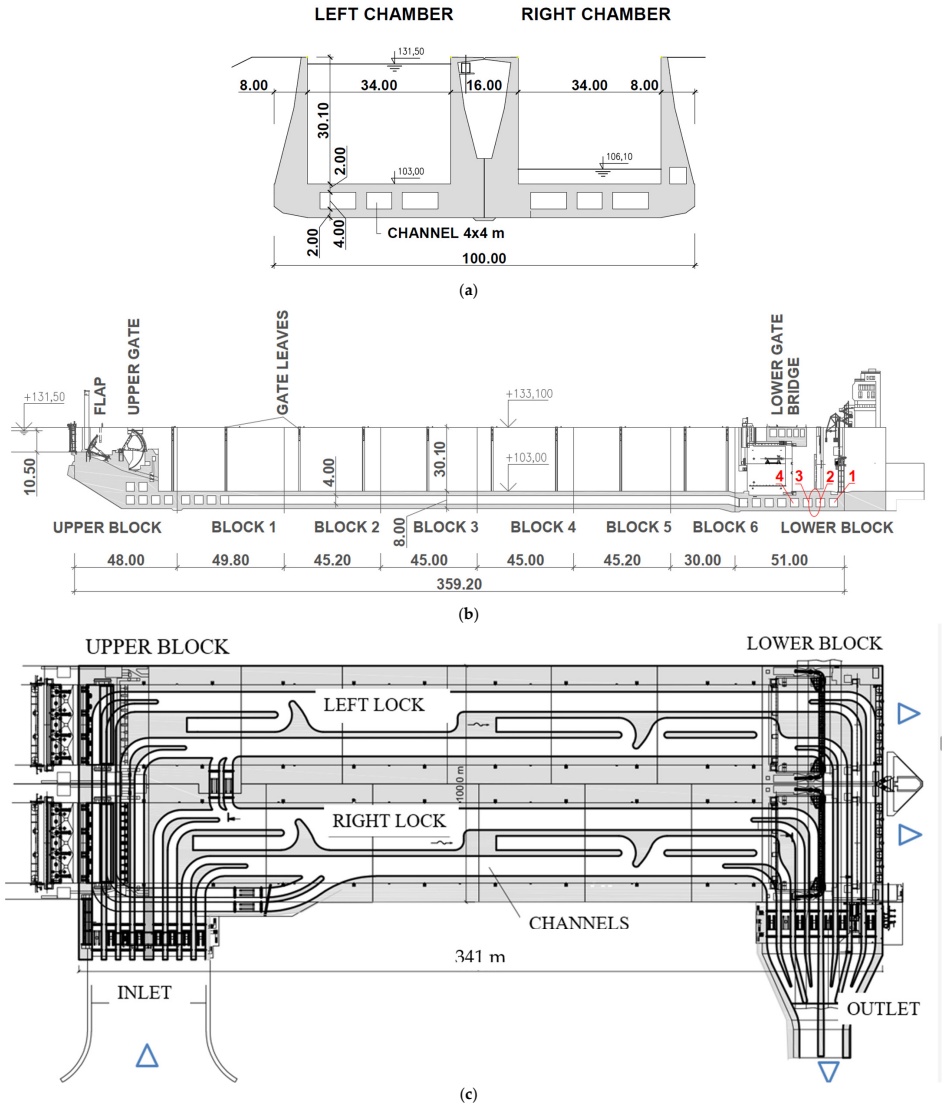


Figure 2. (**a**) Typical cross-section of the lock chambers; (**b**) longitudinal section of the lock; (**c**) general layout of the filling and emptying channels system, with channel markings 1–4 indicated in red.

https://doi.org/10.3390/engproc2026161029

The gate in the upper block can be used to divert ice and to convey flow during floods. The filling and emptying system ensures safe operation of the locks. Eight channels (four for each chamber) are used to convey water into and out of the lock through its bottom. Water is conveyed through slots in the bottom, allowing the lock chamber to fill and empty evenly without creating currents that could endanger vessels within the chamber. It is an indirect filling and emptying system with long bypass channels measuring 4 × 4 m. Each of the eight bypass channels is controlled by two segment valves: one in the inlet structure and one in the outlet structure.

As part of the modernization of the lock chambers, all movable gates had to be replaced. The new anchoring systems for the three main gates—the lower gate, upper gate, and safety flap—are described in detail in Refs. [1,2].

2. Description of the Channel Structure and Observed Damage

The 4 × 4 m channels beneath the lower block form part of a massive concrete structure (Figure 3). The walls, foundation slab, and top slab are 2.0 m thick and are made of C16/20 concrete. The channel walls were reinforced on both faces with Ø25 bars at 200 mm spacing vertically and Ø16 bars at 250 mm spacing horizontally [3]. A construction joint was located between the wall and the top slab.

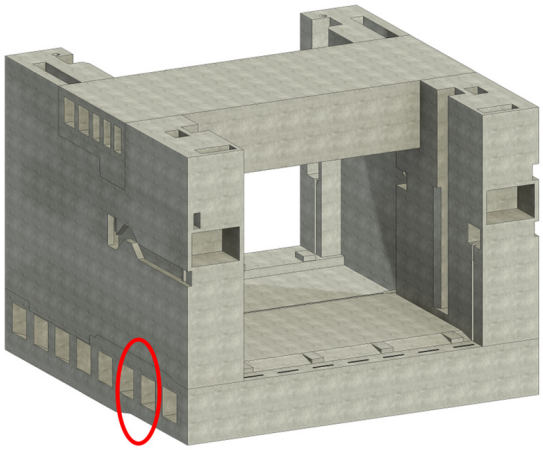


Figure 3. 3D geometry of the lower block highlighting the damaged dividing wall between channels 2 and 3 (indicated in red).

As described above, the lock chambers are filled and emptied through channels located beneath the chamber floor. As shown in Figure 2c, the outlet channels of the left chamber are located beneath the right chamber in plan. The right chamber was reconstructed first, in 2020–2021. The left chamber remained in operation during this period, so these channels could not be visually inspected. The channels were subjected to hydrostatic pressure corresponding to a water head of more than 30 m. After the right chamber was put into operation, the left chamber was closed. During the subsequent inspection of channels 1–4, extensive damage was identified. This damage had not been anticipated in the original reconstruction design. It was therefore necessary to determine the cause of the damage.

Visual inspections conducted from December 2021 to June 2022 revealed extensive damage to the walls of outlet channels 1–4:

- All walls exhibited oblique (shear) cracks originating at the connections between the channel walls and the top and bottom slabs. The largest cracks were observed in the wall between channels 2 and 3 (Figure 3). These major oblique cracks were inclined at approximately 45° and had widths exceeding 1 mm (Figure 4a).

- Other cracks and voids were observed in this wall beneath the top slab and above the bottom slab, essentially along the entire length of the wall. The 150 mm concrete cover was damaged at these locations. Consequently, the construction joint was exposed (Figure 4b).
- At several locations, the Ø25 vertical reinforcing bars were found to be fractured near the top and bottom slabs. At some locations, vertical reinforcing bars were missing near the top slab. Some sections of the reinforcement near the top and bottom slabs could be removed by hand. The fractured bars exhibited flat fracture surfaces without visible necking (Figure 4b).
- The damage to the wall between channels 2 and 3 was assessed as severe.



(**a**) (**b**)

Figure 4. (**a**) Typical diagonal (shear) crack in the dividing wall between channels 2 and 3; (**b**) fractured vertical reinforcement beneath the top slab.

3. Material Properties

Following the discovery of the channel damage, a comprehensive structural investigation was conducted, focusing primarily on determining the material properties of the concrete and reinforcement. The testing laboratory determined the compressive strength of the concrete from core samples taken from the wall between channels 2 and 3. Nine core samples approximately 90 mm in diameter yielded an average compressive strength of 66.7 MPa. Statistical evaluation confirmed that the actual concrete strength corresponded to strength class C40/50 and was therefore significantly higher than the original design specification of C16/20. Consequently, the concrete quality was assessed as excellent.

In addition, three samples of Ø25 mm reinforcement were taken for static and dynamic testing. The static tests yielded an average tensile strength of approximately 600 MPa. Dynamic tests were performed with the stress varying from 0 to 365 MPa at a frequency of 2.5 Hz. The three samples failed after 70,900, 89,800, and 58,100 cycles, respectively. These values are relatively low and are comparable to the approximately 58,300 filling and emptying cycles experienced by the chamber during about 30 years of operation. Furthermore, the fatigue fracture morphology of the tested reinforcement was identical to that of the reinforcement fractures observed at the top slab-to-wall construction joint, with both showing a complete absence of necking (Figure 5). This high degree of similarity strongly indicates that fatigue loading of the reinforcement played a primary role in the observed damage to the channel walls.

https://doi.org/10.3390/engproc2026161029



Figure 5. Fatigue failure morphology of the Ø25 mm reinforcement bars after high-cycle dynamic testing.

4. Structural Analyses

A review of the original structural calculations revealed that the specific loading condition occurring during the reconstruction of the right chamber had not been verified—namely, the scenario with an empty right lock chamber and a full left lock chamber. Under this condition, channels 1–4 are subjected to significant internal hydrostatic pressure corresponding to a water head exceeding 30 m, while the empty right chamber above provides no counteracting hydrostatic pressure. Consequently, the channel walls are subjected to significant vertical tensile forces, which can induce uplift of the top slab. Based on these findings, the structural behavior of the lower block was assessed using the available documentation. Several numerical models were developed to evaluate the stresses in the channel walls:

Model A: 2D cross-sectional models of the damaged dividing wall between channels 2 and 3:

- Linear elastic cross-sectional model developed in SCIA Engineer 22 [5].
- Nonlinear cross-sectional model developed in IDEA StatiCa Detail 22.0 [6] (Figure 6a).
- Nonlinear cross-sectional model developed in ATENA 5.9.0 [7] (Figure 6b,c).

Model B: Global 3D linear elastic model of the entire structure developed in ANSYS LS-DYNA 971 [8] (Figure 6d).

The 2D cross-sectional models (Model A) were used to investigate the fundamental behavior of the most severely damaged wall and to verify the structural design. These models represent a 6.0 m wide structural section with a standard channel clearance of 4.0 × 4.0 m and hydrostatic pressure acting over the 4.0 m channel width.

The global 3D model (Model B) was used to evaluate the tensile stresses in other segments of the lower block and to capture differences in structural behavior among the individual channel walls. The primary advantage of this 3D approach lies in its ability to incorporate the actual geometry of the entire dilatation block, including all niches, shafts, and internal channels.

Although a comprehensive description of these models exceeds the scope of this paper, an extensive parametric study was conducted. This study encompassed various numerical approaches (linear and nonlinear, 2D and 3D), with different boundary conditions and concrete strength classes considered to evaluate potential structural risks. The mechanical behavior and contact conditions at the construction joint were also thoroughly investigated. According to current structural standards, all numerical models indicated that the structure did not satisfy the requirements for either the ultimate limit state (ULS) or the serviceability limit state (SLS). Crucially, the models reproduced a failure mode that was highly consistent with the actual damage observed on-site.

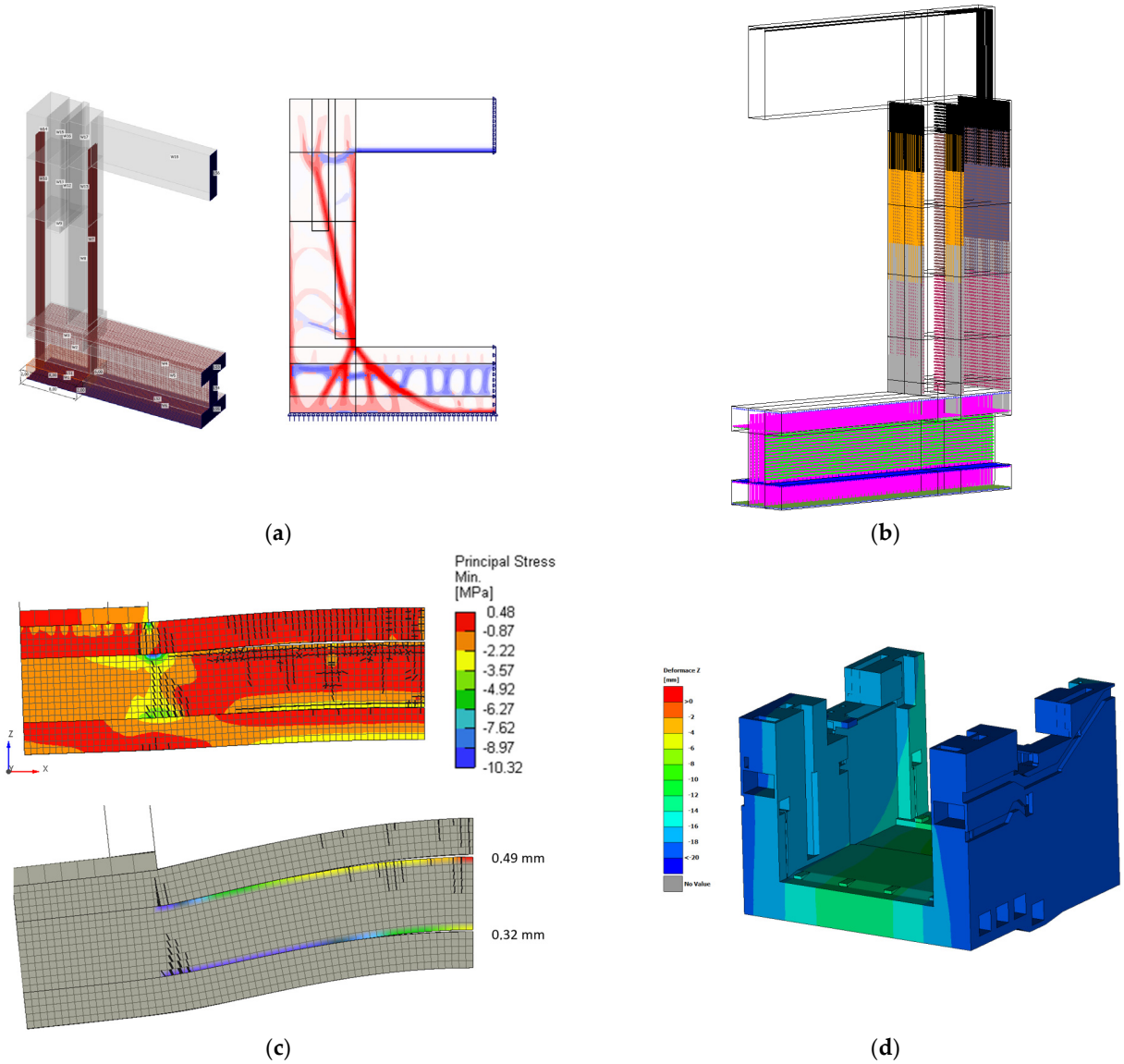


Figure 6. Numerical modeling results: (**a**) Nonlinear Model A (IDEA StatiCa Detail) showing reinforcement layout and the strut-and-tie mechanism (compression in red, tension in blue); (**b**) Nonlinear Model A (ATENA) reinforcement layout; (**c**) principal tensile stresses and joint displacement showing the opening of the construction joint under internal overpressure; (**d**) global 3D linear elastic model (ANSYS) of the lower dilatation block.

As illustrated in Figure 6a, the model reproduces the observed trajectory of the shear cracks and shows the stress distribution at the wall-to-slab interfaces. The numerical analysis demonstrated a clear tendency for the construction joint between the top slab and the wall to open (Figure 6c), with the resulting joint opening leading to failure of the reinforcement crossing the joint. It is evident that the unbonded construction joint is incapable of transmitting tensile stresses. Consequently, the entire tensile demand must be resisted solely by the reinforcement under all relevant design conditions, including ULS, SLS, and fatigue. Therefore, rehabilitation and strengthening of the channel walls were urgently recommended. Furthermore, if water penetrates the open construction joint, the hydrostatic load increases substantially (by 50%), further increasing the stresses in the reinforcement.

https://doi.org/10.3390/engproc2026161029

5. Channel Wall Strengthening

The need to strengthen the outlet channel walls significantly disrupted the schedule of the originally planned lock modernization. The proposed strengthening scheme uses high-strength prestressing bars installed in bored holes (Figure 7a) [9]. These Ø36 mm bars are installed at 0.8 m center-to-center spacing. This configuration provides continuous vertical post-tensioning across all structural elements, thereby inducing a compressive stress state within the construction joint beneath the top slab. Consequently, the fatigue stress amplitude in the existing reinforcement will be significantly reduced.

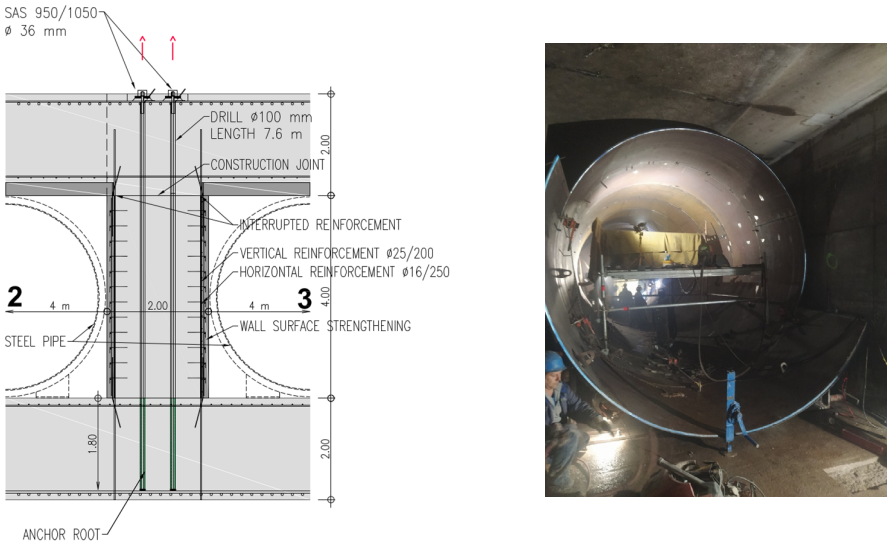


Figure 7. Structural rehabilitation schemes: (**a**) post-tensioning principle for the dividing wall between channels 2 and 3 using prestressing bars; (**b**) installation of the temporary steel pipeline bypass inside the 4 × 4 m channels.

The installation process requires drilling vertical boreholes approximately 8.0 m deep. A 1.8 m long roughened anchorage zone is provided at the bottom of each borehole to ensure adequate bond strength. Once the bars are post-tensioned, the boreholes are fully grouted. However, implementing this permanent strengthening scheme required the simultaneous closure of both lock chambers. Specifically, the channel walls of the left chamber could only be drilled while the adjacent right chamber was empty. This scenario would have resulted in a complete suspension of navigation on the Danube River, which was unacceptable for operational and economic reasons. Continuous operation of at least one lock chamber was therefore required.

To overcome this constraint, a temporary solution was proposed for a transitional period of approximately 2–3 years, enabling completion of the reconstruction of the left chamber. This interim measure involved installing a temporary steel pipeline with a diameter of nearly 4.0 m directly inside channels 2 and 3 (Figure 7b). This steel bypass safely withstands the entire internal hydrostatic overpressure, thereby substantially reducing the stresses in the concrete channel walls. Concurrently, selected damaged walls in the left chamber channels were locally strengthened with prestressing bars. This temporary system was implemented in 2023, allowing the modernization of the lock chambers to proceed. Consequently, it will now be possible to temporarily decommission the right chamber and carry out the permanent post-tensioning of the damaged channel walls, with this work scheduled for the coming year.

6. Conclusions

This paper presented an investigation into an unusual structural failure of reinforced concrete hydraulic channels subjected to high internal water pressure. A comprehensive forensic engineering investigation and damage assessment were carried out. A series of linear and nonlinear numerical analyses identified the causes of the observed damage and provided the basis for the development of both temporary and permanent rehabilitation strategies. The case highlights the importance of considering construction joints and fatigue effects in reinforced concrete hydraulic structures subjected to repeated high internal pressure.

Author Contributions: Conceptualization, M.Z. and M.T.; methodology, M.Z.; software, O.Š. and M.L.; investigation, O.Š. and M.Z. and M.L.; resources, M.Z.; data curation, O.Š.; writing—original draft preparation, M.Z. and O.Š. and M.L.; writing—review and editing, M.T.; project administration, M.Z. and M.T.; funding acquisition, M.Z. All authors have read and agreed to the published version of the manuscript.

Funding: This article was was supported by the BUT project no "FAST-S-26-8945 Advanced Analyses of Existing Concrete and Masonry Structures." The theoretical foundations presented in the article were carried out with financial support from the state budget, provided via the Technology Agency of the Czech Republic (TA ČR) under project no. CL02000084, Development of a Comprehensive Prefabricated System for Constructing Cycle Paths on Disused Railway Lines, with the Potential for Restoring Railway Traffic.

Institutional Review Board Statement: Not applicable.

Informed Consent Statement: Not applicable.

Data Availability Statement: The data supporting the findings of this study are available from the corresponding author upon reasonable request.

Conflicts of Interest: Author Michael Trnka was employed by the company Aquatis, a.s. The remaining authors declare that the research was conducted in the absence of any commercial or financial relationships that could be construed as a potential conflict of interest.

References

1. Zich, M.; Trnka, M.; Šimek, O.; Skalník, S. Innovation and modernization of Gabčíkovo lock chambers. In Proceedings of the 14th Central European Congress on Concrete Engineering, Vodice, Croatia, 22–24 September 2024; p. 124, ISBN 978-80-908943-1-0.
2. Zich, M.; Trnka, M.; Šimek, O. Innovation and Modernization of Gabčíkovo Lock Chambers. *Struct. Concr.* **2025**, *26*, 4015–4029. [CrossRef]
3. Hydroconsult Bratislava. *The Original Project of the Lock Chambers—Concrete Structures*; Technical Report; Hydroconsult: Bratislava, Slovakia, 1985.
4. *EN 1992-1-1:2023*; Eurocode 2: Design of Concrete Structures—Part 1-1: General Rules and Rules for Buildings, Bridges and Civil Engineering Structures. European Committee for Standardization: Brussels, Belgium, 2023.
5. SCIA Group. *SCIA Engineer 22*; SCIA Group: Hasselt, Belgium. Available online: www.scia.net (accessed on 5 September 2026).
6. IDEA StatiCa. *IDEA StatiCa Detail Documentation*, version 22.0; IDEA StatiCa: Brno, Czech Republic. Available online: www.ideastatica.com (accessed on 5 September 2026).
7. Červenka, V.; Jendele, L.; Červenka, J. *ATENA Version 5.9.0 Program Documentation: Part 1 Theory*; Červenka Consulting: Prague, Czech Republic, 2016. Available online: http://cervenka.cz (accessed on 5 September 2026).
8. ANSYS, Inc. *ANSYS LS-DYNA*, Version 971; ANSYS, Inc.: Canonsburg, PA, USA, 2021. Available online: https://www.ansys.com/products/structures/ansys-ls-dyna (accessed on 5 September 2026).
9. AQUATIS Brno a.s. *Project Documentation of Innovation and Modernization of Gabčíkovo Lock Chambers*; Technical Report; AQUATIS: Brno, Czech Republic, 2019–2023.

Disclaimer/Publisher's Note: The statements, opinions and data contained in all publications are solely those of the individual author(s) and contributor(s) and not of MDPI and/or the editor(s). MDPI and/or the editor(s) disclaim responsibility for any injury to people or property resulting from any ideas, methods, instructions or products referred to in the content.